ACS APPLIED MATERIALS & INTERFACES

Article

Fabrication of Surface Protein-Imprinted Biofuel Cell for Sensitive Self-Powered Glycoproteins Detection

Jiang Ouyang, Zhenjun Liu, Yajing Han, Ke Zeng, Jianping Sheng, Liu Deng, and You-Nian Liu

ACS Appl. Mater. Interfaces, **Just Accepted Manuscript** • DOI: 10.1021/acsami.6b12010 • Publication Date (Web): 01 Dec 2016

Just Accepted

ACS Publications

ACS Applied Materials & Interfaces is published by the American Chemical Society.
1155 Sixteenth Street N.W., Washington, DC 20036

Fabrication of Surface Protein-Imprinted Biofuel Cell for Sensitive Self-Powered Glycoproteins Detection

Jiang Ouyang,[†] *Zhenjun Liu,*[†] *Yajing Han,*[†] *Ke Zeng,*[†] *Jianping Sheng,*[†] *Liu Deng,*[*,†] *and You-Nian Liu*[*,†]

College of Chemistry and Chemical Engineering, Central South University, Changsha, Hunan 410083, PR China

ABSTRACT: Glycoproteins are important biomarkers and therapeutic targets in clinical diagnostics. The conventional analytical methods for glycoprotein are usually faced some challenges such as the complex pretreatment of samples, poor availability and limited stability of antibody, making them not suitable for point-of-care and on-site application. Herein, we demonstrate a novel miniaturized biofuel cells (BFCs)-based self-powered nanosensor for the specific and sensitive determination of glycoproteins in complex samples through the combination of boronate-affinity molecularly imprinted polymer (MIP) and the boronate-affinity-functionalized biliroxidase/carbon nanotube nanocomposites. The above MIP and the nanocomposites act as both signal probe and biocatalyst at the cathode. The as-obtained self-powered MIP-BFC-based biosensor can detect horseradish peroxidase (a type of glycoprotein) with a wide linear range of 1 ng/mL to 10 μg/mL and a very low detection limit of 1 ng/mL. Especially, it shows high tolerance for

[*]Corresponding authors: Phone (Fax):+86-731-8887 9616. E-mail: dengliu@csu.edu.cn (L. Deng); liuyounian@csu.edu.cn (Y.-N. Liu).

different interferences (*e.g.* sugars and other glycoproteins), and can even measure the α-fetoprotein level in serum samples. Moreover, it exhibits significant advantages over the conventional assays in terms of cost efficiency, stability and speed, especially inexpensive instrument needed. Our novel approach for construction the sensor paves a simple and economical way to fabricate portable device for point-of-care and on-site application.

KEYWORDS: biofuel cell, protein imprinted polymer, glycoprotein, biosensor, self-power

1. INTRODUCTION

Glycoproteins play an important role in regulating the biological processes such as bacterial pathogenesis, inflammation and cancer cell metastasis.[1,2] They are of great significance as cancer biomarkers, which can convey information about the physiological state of the cells, for clinical diagnosis.[3,4] To date, various methods have been explored to detect and quantify glycoproteins, including mainly mass spectrometry,[5] immunoassay,[3] electrophoresis[4] and affinity chromatography.[6] However, some of the above mentioned methods require expensive agents, complicated operation and extra powered instruments, making them not suitable for point-of-care and on-site application. Recently, self-powered sensors based on biofuel cells (BFCs), along with the efficiency of electrochemical energy conversion with the biocatalytic property of biocatalyst, are drawing enormous attention.[7–10] Due to the capability for the detection without external power sources, simplifying the fabrication, minimizing the scale and reducing the cost, the self-powered biosensors based on BFCs are considered to be especially beneficial for the miniaturization of detection for point-of-care and on-site application in near future. Followed by the first BFCs-based self-powered sensors,[11] BFCs-based self-powered system has been used as sensitive and selective method for the detection of cysteine,[12] cyanide,[13] acetaldehyde,[14] cell,[15] explosives[16] and *etc*. These previous studies indicate considerable promise in analytical systems. However, they are restricted to the modulator or substrate of the biocatalyst utilized in BFC. To broaden the application scopes, antibody-antigen,[17–19] DNA[20] and aptamer-protein[21] have been incorporated

into the electrochemical interface for adjusting the power output of BFCs. Despite the impressive performance, the fabrication requires either expensive indigents or complicated manipulations, which seriously limits the point-of-care and on-site application of new-concept self-powered biosensors. Therefore, a novel strategy that allows facile and efficient engineering of sensing elements onto the BFC without affecting power generation while maintaining the performance of sensors is highly desirable and demanded.

Molecularly imprinted polymers (MIPs) with the specific binding affinity for biological receptors, are of great interest for the development of highly selective sensors. Based on the reversible covalent binding between boronic acid and sugar, MIPs have been designed to specifically recognize proteins through Raman, fluorescence or chemiluminiscence and *etc*.[6,22–24] The boronate-affinity MIPs can offer a greater stability, lower cost and better engineering opportunity than traditional biological receptors, such as antibody and aptamer, thus making them appealing alternatives to antibodies or aptamer for bioassays.[25,26] In this regard, the combination of MIPs with BFCs may generate new analytical approaches that outperform the conventional immunoassays.

Herein, we demonstrate a new concept on an integration of boronate-affinity MIPs and BFCs for developing new miniaturized BFCs-based self-powered sensors for the specific and sensitive determination of trace glycoprotein in complex samples. The design of such molecularly imprinted polymer-based self-powered sensor is conceptually new, through a great challenge is still existed to date because it is very

difficult to realize the molecular recognition ability and the efficient power output at the same time. This interesting sensing system relies on the combination of the boronate-affinity MIPs and the boronate-affinity-functionalized BOD/CNT nanocomposites, where MIPs act as the recognition unit for glycoprotein, while the nanocomposites serve as a signal probe and biocatalyst at the cathode of BFCs. The obtained sensor can detect horseradish peroxidase (HRP, a type of glycoprotein) with a wide linear range of 1 ng/mL to 10 μg/mL, and shows high tolerance for various interferences (*e.g.* sugars and other glycoproteins). To demonstrate the clinical relevance of our self-powered biosensor, the level of α-fetoprotein (AFP) in serum samples was measured, well in accordance with commercial ELISA analysis.

2. EXPERIMENTAL SECTION

2.1. Materials. Carbon nanotubes (CNTs) were purchased from Shenzhen Nanotech Port (Shenzhen, China), further treated with mixed acids (HNO_3 and H_2SO_4) to get –COOH group on their surface. Bilirubin oxidase (BOD) from Myrothecium verrucaria, lyophilized 99% bovine serum albumin (BSA), 1-ethyl-3-(3-dimethyllaminopropyl) carbodiimide hydrochloride (EDC), *N*-hydroxysuccinimide (NHS), KH_2PO_4 and K_2HPO_4 were purchased from Sigma-Aldrich (St. Louis, MO, USA). Polyethylene glycol 200 (PEG-200) (average molecular weight, 190.0 – 210.0) was purchased from Alfa Aesar (Ward Hill, MA, USA). Benzoin dimethyl ether was obtained from Aladdin Reagent (Shanghai, China). Horseradish peroxidase (HRP), ribonuclease B (RNase B) from bovine pancreas, ribonuclease A (RNase A) from bovine pancreas, cytochrome C (Cyt C), myoglobin

(Myo), bovine serum albumin (BSA), apo-transferrin (Trans), hemoglobin (Hemo), albumin from chicken egg white (OVA), *D*-glucose, human apo-transferrin (TRF), and γ-methacryloxypropyltrimethoxysilane (γ-MAPS), 4-aminophenylboronic acid (APBA) were all from Sigma-Aldrich (St. Louis, MO, USA). Polyethylene glycol diacrylate (PEGDA) (average molecular weight, 258), 4-vinylphenylboronic acid (VPBA) and anhydrous methanol were purchased from Beijing Reagent Co. (Beijing, China). Sodium dodecyl sulphate (SDS) was obtained from Bio-Rad (Hercules, CA, USA). Human α-fetoprotein (AFP) was purchased from Shuangliu Zhenglong Biology and Chemistry Research Institute (Chengdu, China). All these reagents were used without further purification. Other chemicals were of analytical grade or higher. HPLC-grade methanol was from Merck (Darmstadt, Germany).

2.2. Fabrication of MIP modified electrode. The MIP modified electrode was prepared according to the previously reported method.[23] First, to silanize the glassy carbon (GC) electrode, the cleaned GC electrode was immersed in a 1:9 (v/v) mixture of γ-MAPS and methanol at 60 °C for 8 h. Then the silanized electrode was rinsed with methanol and water to remove the residual reagents. To prepare the HRP-imprinted MIP, 1 mg VPBA and 100 μL PEG-200 were dissolved in 94 μL Na_2HPO_4 aqueous solution (0.2 M, pH 9.3). After sonicated for 5 min, 6 μL HRP solution (10 mg/mL), 1 mg benzoindimethyl ether, 300 μL PEG-200 and 100 μL PEGDA were added to the mixture and stirred for 10 min. The obtained solution was coated onto the silanized electrode. The electrode was then irradiated by UV curing for 20 s. After washed with an acetonitrile/water mixture (30:70, v/v) for 30 min, the

resulting electrode was finally immersed in a 0.2 M H_3PO_4 solution containing 30% acetonitrile (v/v) for 2 h to extract the imprinted HRP template. For preparation of AFP MIP electrode, 6 μL of the AFP solution (10 mg/mL in 0.1 M PBS, pH 7.5) was added into the mixture as template molecule instead of HRP solution, and the following steps are identified as those for HRP. For the preparation of non-imprinted polymer (NIP) electrode, the protein template solution was replaced by pure water of identical volume, and the preparation procedures were the same as those for HRP MIP electrode.

2.3. Preparation of the APBA/CNT/BOD nanocomposites.

To prepare the electrochemical signal probe, 50 μL of 0.5 M NHS, 50 μL of 1 M EDC, 50 μL of 6 μM APBA and 10 μL of 12 mg/mL BOD aqueous solutions were added into 500 μL 1 mg/mL CNT solution in sequence, then the mixture was stirred in a small vial overnight. After the completion of the reaction, the reaction mixture was centrifuged at 10,000 rpm at 4 ^{o}C for 15 min, and the supernatant was discarded to remove any free BOD and APBA. The above wash process was repeated for four times. Finally, 100 μL PBS (0.01 M, pH 7.0) was added to the collected precipitate to form a homogeneous dispersion. The solution was stored at 4 ^{o}C and diluted with PBS before use. The APBA/CNT was fabricated in the same way but without the addition of BOD in the first step.

2.4. Preparation of MIP/HRP/APBA/CNT/BOD electrode.

To fabricate the biocathode, the HRP-MIP electrode was immersed into the HRP solution with different HRP concentrations for 20 min to capture HRP. Then the

electrode was washed with water to get rid of any loosely absorbed HRP. Then the HRP-MIP electrode was immersed into a signal probe (APBA/CNT/BOD nanocomposites) solution for 2 min to label the pre-captured HRP. The obtained MIP/HRP/APBA/CNT/BOD electrode was washed with water and blown to dry by nitrogen. The MIP/HRP/APBA/CNT electrode was fabricated by incubating the HRP-MIP electrode into HRP and APBA/CNTs solution in sequence. For the preparation of APBA/CNT/BOD/HRP-NIP electrode, the MIP electrode was replaced by NIP electrode, and the other steps were the same as those of APBA/CNT/BOD/HRP-MIP electrode. Then, the measurement of above electrodes toward oxygen reduction was carried out in air-saturated quiescent PBS (0.2 M, pH 7.5).

2.5. Optimization of MIP/HRP/APBA/CNT/BOD electrode performance.

The evaluation of MIP/HRP/APBA/CNT/BOD electrode performance was performed by using the oxygen reduction polarization current of the prepared electrode at 0.4 V in presence of 100 μg/mL HRP. To optimize the amount of APBA used for the APBA/CNT/BOD electrochemical signal probe, 50 μL of different concentrations of APBA (2 μM, 4 μM, 8 μM, 12 μM, 16 μM, 20 μM) and 10 μL of 5 mg/mL BOD were added to 500 μL of 0.5 mg/mL CNT solution. And the mixture was stirred overnight at room temperature. Then, the optimized APBA concentration was fixed, while different concentrations of BOD (1, 3, 6, 9, 12, 15 and 18 mg/mL) were adopted. The oxygen reduction performance of APBA/CNT/BOD

nanocomposites was evaluated using the polarization current of the prepared biocathode at 0.4 V in presence of 100 μg/mL HRP.

2.6. Preparation of thionine/graphene/GDH electrode.

The thionine/graphene/GDH electrode was fabricated according to our previous work with little modification.[28] Briefly, the thionine/graphene nanosheets was fabricated by mixing 20 mL of 0.5 mg/mL homogeneous suspension of graphene and 20 mL of 0.2 mM thionine aqueous solution. After being vigorously shaken or stirred for 30 minutes, the stable dark green species were collected by centrifugation at 10,000 rpm for 20 min. The obtained thionine/graphene nanosheets was washed with water for at least three times. Then 100 μL of 5 mg/mL GDH (in PBS, pH 7.4) was mixed with 100 μL thionine/graphene suspension (0.25 mg/mL) and stirred for 5 min. For the preparation of thionine/graphene/GDH modified electrode, 5 μL of the resultant thionine/graphene/GDH nanocomposites was dropped onto the surface of carbon electrode, and dried at 4 ^{o}C overnight. The graphene electrode was fabricated by dropping the graphene onto the carbon electrode directly. The graphene/GDH composites were obtained by mixing 100 μL of GDH (5 mg/mL in PBS, pH 7.4) and 100 μL of graphene suspension (0.25 mg/mL) in the absence of thionine. Finally, the graphene/GDH modified anode was prepared by dropping 5 μL of the graphene/GDH mixture to the carbon electrode surface.

2.7. Fabrication of miniaturized printed carbon-based BFCs.

The miniaturized printed carbon electrode chips with two electrodes were prepared on the plastic plates by using standard microfabrication technique.[25] The

MIP/HRP(AFP)/APBA/BOD/ CNT electrode was applied as the biocathode. For the preparation of the biocathode, a PDMS layer with a cavity, which is the same size as one printed carbon electrode (3 mm × 3 mm × 60 mm), was first covered on one electrode surface. Then all the modification processes for the printed carbon electrode of MIP/HRP(AFP)/APBA/ BOD/CNT were carried out inside of this cavity. MIP carbon electrode was obtained as the same step as mentioned in the section 2.2. The vinyl silanization of the printed carbon electrode was carried out by incubating in γ-MAPS and methanol mixture for 8 h, then the pre-polymer solution, which was prepared as the above mentioned in section 2.4, was dropped on the silanized carbon electrode then covered with an appropriate photomask. After irradiation under UV light for 20 s, the PDMS layer was removed, and the electrode was washed by the acetonitrile/water mixture (30:70, v/v) to remove the unreacted component and the template (HRP). The resulting MIP carbon electrode was covered by PDMS layer again. For the fabrication of MIP/HRP(AFP)/APBA/CNT/BOD electrode, the glycoprotein (HRP or AFP) capture and the APBA/CNT/BOD nanocomposites labelled processes were carried out follow the same procedures in section 2.4. The thionine/graphene/GDH electrode was utilized as the bioanode. Finally, 5 μL thionine/graphene/GDH nanocomposites was dropped onto another printed carbon electrode and dried at the 4 ^{o}C overnight to fabricate the bioanode. To assemble a fuel cell, the two above electrodes were connected through an external 50 Ω resistor.

2.8. Measurement of glycoprotein by MIP-BFCs-based self-powered sensors.

To measure the HRP concentration, the MIP electrode with HRP template was used as the basement for the biocathode. First, the MIP electrode was covered by a PDMS cell with a cavity, which is the same size as MIP electrode. Then a series of HRP solution was added into the PDMS cavity and was captured on the HRP-MIP electrode. After washed with water, APBA/CNT/BOD nanocomposites solution was added into the PDMS cavity, and labelled on the HRP. After BFC were fabricated, a PDMS cell with a round cavity with dimensions of 10 mm and height of 60 mm covered on the two modified electrodes. Then the MIP/HRP/APBA/CNT/BOD biocathode was connected through an external 50 Ω resistor to the thionine/graphene/GDH bioanode. For the investigation of the performance of BFC, the electrolyte (10 mM NAD^+, 15 mM glucose and at pH 7.5 in air-saturated quiescent solution) was added into the PDMS cell. Then the current and potential output of the BFC system for different HRP concentrations were measured by using a digital multimeter (Keithley 2700).

2.9. Selectivity of the MIP-BFCs-based self-powered sensors. The cross-reactivity experiment was performed with HRP-templated MIP-BFCs toward a variety of proteins, including Cyt C, RNase A, RNase B, Myo, OVA, Hemo, BSA and HRP. 20 μL of 1 μg/mL specific protein dissolved in 0.1 M PBS (pH 7.4) was added onto PDMS cell and incubated for 20 min in a humidity chamber. After wash with water, the captured glycoprotein modified biocathode was further treated with APBA/CNT/BOD by incubating electrode with 5 μL of APBA/CNT/BOD for 2 min. The cross-reactivity was roughly estimated in terms of the percentage of the intensity

of interfering proteins over the intensity of HRP under identical concentrations. The interference experiment was conducted with HRP-templated MIP-BFC toward 20 μL 1 μg/mL HRP with additional 1 mg/mL BSA, 1 mg/mL Hemo and 1 mg/mL OVA. The protein mixture was added onto PDMS cell, and the following measurement process is the same as those for HRP. We also tested the effect of high-concentration glucose on the detection of HRP. In this case, the sample was a mixture of 1 μg/mL HRP and 1g/L glucose.

2.10. Assay of AFP in human serum by MIP-BFCs-based self-powered sensors. To assess the practical application of the MIP-BFCs-based self-powered sensors, the detection of total AFP in serum was conducted as follows. The AFP-imprinted MIP-BFC was executed as the same steps as those of the HRP-imprinted MIP electrode except for using AFP as imprinted template. Human serum was diluted 20-fold with PBS (pH 7.0) and then spiked with AFP of known concentrations. A 20 μL of serum sample was added to the cathode cell for 20 min in a humidity chamber. After washing with water, the captured glycoprotein was labelled by incubating with 5 μL of APBA/CNT/BOD nanocomposites for 2 min. The MIP/AFP/APBA/CNT/BOD biocathode was further connected to the bioanode. Then the power output of the AFP imprinted MIP-BFC was measured in electrolyte air-saturated quiescent solution with 10 mM NADH and15 mM glucose at pH 7.5 (0.2 M PBS).

2.11. Calculation of imprinting efficiency and imprinting factor. Based on the information provided by the adsorption isotherm as well as the experimental

conditions used, the imprinting efficiency and imprinting factor were calculated according to the following equations:

$$I_E = (Q_{MIP} - Q_{NIP})/Q_p \quad (1)$$

$$I_F = Q_{MIP}/Q_{NIP} \quad (2)$$

where I_E and I_F are imprinting efficiency and imprinting factor, respectively; Q is the saturated adsorption capacity obtained directly from the adsorption isotherm, the subscript indicates MIP or NIP, Q_p is the concentration of the template in the pre-polymer solution used for the preparation of the MIP.

2.12. Characterizations. The electrochemical measurements of bioelectrodes were performed by using a Chenhua CHI 660 Electrochemical system (Shanghai, China). Coiled platinum wire and an Ag/AgCl (saturated KCl) electrode were used as the counter electrode and the reference electrode, respectively. Current and potential output of the biofuel cells system were measured by using a digital multimeter (Keithley 2700). We connected the two electrodes through an external 50 Ω resistor for assessment of the BFC performance. All tests were conducted at 30 °C. Transmission electron microscopy (TEM) images were obtained with a Hitachi H-600 microscope (Hitachi, Japan). Scanning electron microscopic (SEM) characterization was recorded on a FE-SEM S-4800 system (Hitachi, Japan).

3. RESULTS AND DISCUSSION

3.1 Characterization of the MIP electrode

The boronate-affinity MIP was first prepared *via* the established protocol, due to its facile and easy production.[24] The procedure of MIP modified electrode to recognize

the glycoprotein is shown in **Scheme 1a.** SEM image of boronate-affinity MIP (**Figure S1**) shows that the boronate-affinity MIP has a similar structure to the reported one.[24] Thus, the target glycoprotein in the sample could be captured by MIP electrode through the boronate-sugar affinity. At the same time, the boronate-affinity BOD/CNT nanocomposites was prepared by the modification of BOD/CNT with 4-aminophenylboronic acid (APBA), according to the **Scheme 1b**. TEM image of boronate-affinity BOD/CNT nanocomposites is shown in **Figure S2**. It can be observed that after the CNT nanocomposite was further linked with BOD and APBA, there is a thin layer with 5 nm thickness covered on the surface of CNT, indicating that BOD was bound on the surface of CNTs. As shown in **Scheme 1c**, the obtained APBA/CNT/BOD nanocomposite can be labelled on the captured glycoprotein by the boronate-sugar affinity, while BOD, which acts as the electrochemical probe in the BFC based sensor, can facilitate the oxygen reduction.

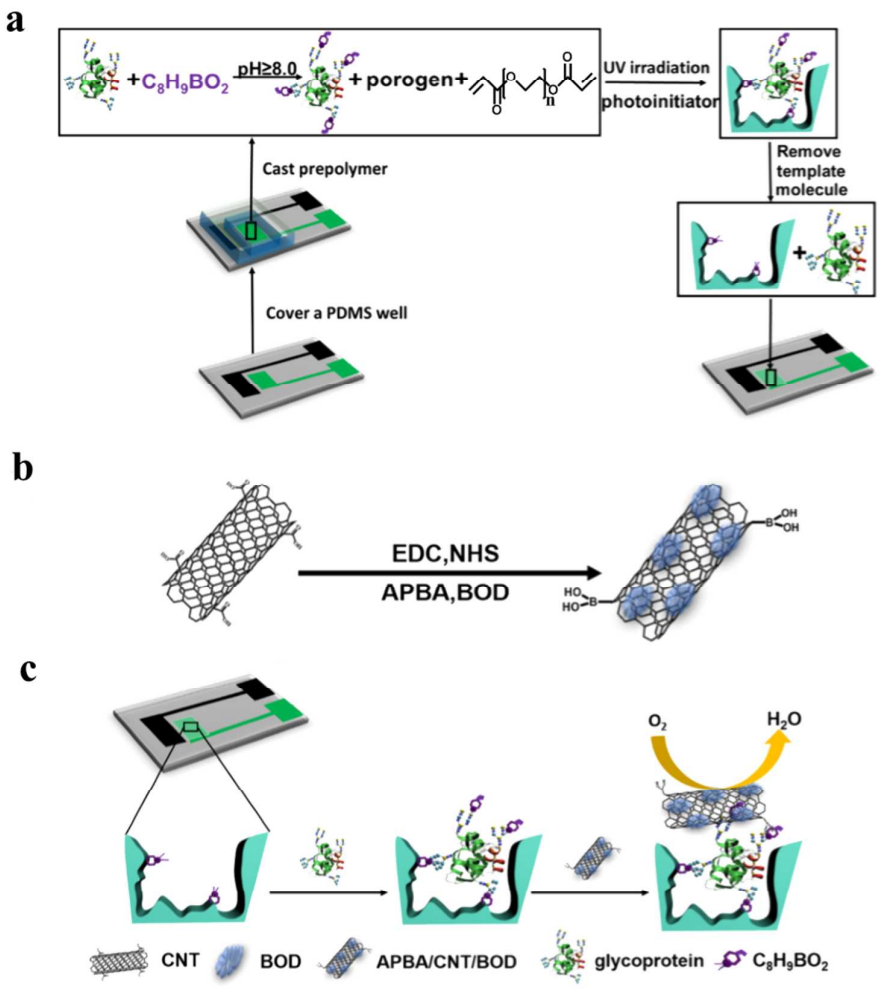

Scheme1 (a) The fabrication procedure of the boronate-affinity MIP modified electrode; (b) The preparation of the APBA/CNT/BOD nanocomposites; (c) The principle of the MIP electrode for the glycoprotein recognition and oxygen reduction.

Herein, HRP was first employed as a model glycoprotein to examine the sensing performance of the MIP-BFCs. To evaluate the performance of the MIP-based cathode, we conducted the electrochemical measurements of the MIP-based cathode in a three-electrode cell, using platinum foil as a counter electrode and Ag/AgCl (saturated KCl) as a reference electrode in the absence or presence of oxygen at pH 7.0 (PBS). After 100 ng/mL HRP was captured by boronate-affinity MIP and further

linked by the APBA/CNT/BOD nanocmoposite, the resulting biocathode exhibits excellent bioelectrocatalytic activity for the reduction of oxygen at 0.54 V (*vs.* Ag/AgCl) in the absence of mediator (**Figure 1a**). This value is close to the redox potential of the T1 Cu site, which is the most plausible electron-accepting site of BOD.[16, 27] The results indicate that BOD immobilized on MIP-cathode can work as an efficient DET-type biocatalyst for O_2 reduction. The control experiments in the absence of BOD were performed under the same conditions. No obvious catalytic currents for O_2 reduction were observed at the MIP, MIP/HRP and MIP/HRP/APBA/CNT modified electrodes (**Figure S3**), demonstrating that HRP is not able to catalyze directly O_2 reduction on the electrode, and only BOD immobilized on MIP-cathode can work as an efficient biocatalyst for O_2 reduction. We also found that the catalytic peak current increases with increasing the amount of target (HRP) (**Figure 1b**), suggesting that the MIP-biocathode has a good potential in the development of new-concept self-powered MIP sensors.

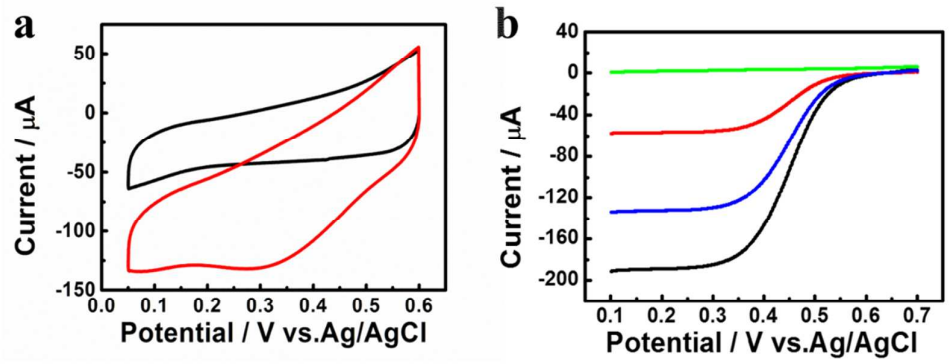

Figure 1. (a) CVs of MIP/HRP/APBA/CNT/BOD electrode in a nitrogen-saturated (black line) and air-saturated (red line) solution at pH 7.0 in the presence of 10 μg/mL HRP; and (b) Polarization curves of MIP/HRP/APBA/CNT/BOD electrode in

air-saturated solution at pH 7.0 in the absence of HRP (green line) and presence of 10 ng/mL HRP (red line), 1 μg/mL HRP (blue line) and 100 μg/mL HRP (black line).

3.2. The characterization of the thionine/graphene/GDH. The anode of biofuel cells was designed as follows. First, the thionine/graphene hybrid nanosheets were prepared through π-π stacking and electrostatic interaction (**Figure 2a**). The as-prepared thionine/graphene could serve as a biocompatible matrix for assembling enzyme and a mediator for facilitating the electron transfer between the enzyme and electrode. Using glucose dehydrogenase (GDH) as a model system, we developed an effective anode biocatalyst with NAD^+ as the cofactor for oxidation of glucose. **Figure 2b** shows the electrocatalytic activity of the thionine/graphene/GDH anode toward glucose oxidation in presence of NAD^+. The addition of glucose results in a significant increase in the anodic current at ~0 V because the self-assembly of thionine to graphene surface provides the necessary mediation and conduction pathways and facilitate electrical communication between NAD^+ and the electrode surface. Control electrocatalytic experiments in the absence of GDH or thionine or NAD^+ under the similar conditions revealed that the corresponding electrochemical interfaces cannot effectively catalyze the oxidation of glucose (**Figure 2c&2d**). And the polarization curves of thionine/graphene/GDH anode in PBS containing 20 mM glucose were illustrated in **Figure 2e**. The onset potential of oxidation toward glucose moves to –0.10 V along with the plateau current reaching 161 μA at 0.10 V. The thionine/graphene/GDH anode provides excellent catalytic performance for the glucose oxidation.

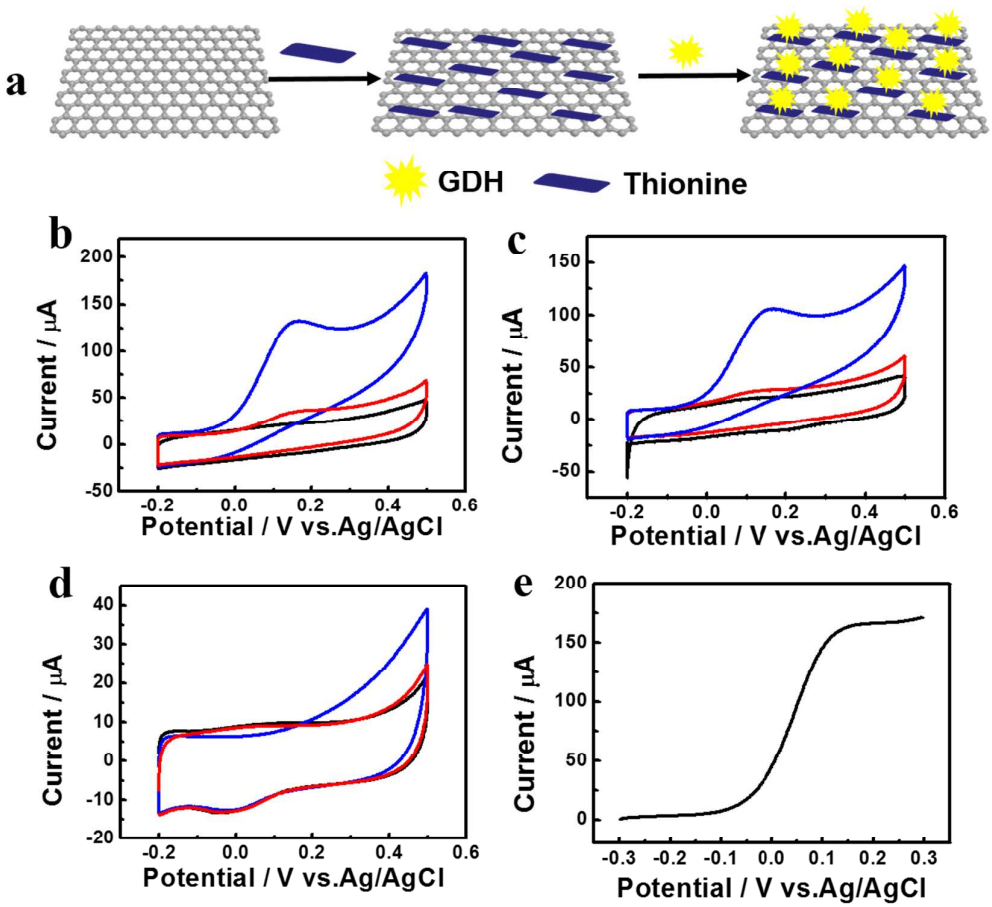

Figure 2 (a) The preparation procedure of the thionine/graphene/GDH nanocomposites. (b) CVs of thionine/graphene/GDH electrode in a PBS (black line), PBS containing 10 mM NAD^+ and 15 mM glucose (blue line), PBS containing 15 mM glucose (red line); (c) CVs of thionine/graphene electrode in a PBS (black line), PBS containing 10 mM NADH (red line) and PBS containing 15 mM glucose (blue line); (d) CVs of graphene electrode in a PBS (black line), PBS containing 10 mM NADH (red line) and PBS containing 15 mM glucose (blue line); (e) Polarization curves of thionine/graphene/GDH electrode in air-saturated PBS containing 20 mM glucose and 5 mM NAD^+ at pH 7.0. All experiments operated in air-saturated PBS at pH 7.0.

3.3. Characterization of the Protein-imprinted Biofuel Cell.

The development of miniaturized devices has been spurred by the desire to produce low-cost point-of-care diagnostics and environmental monitoring devices. Due to the presence of BOD, the resulting MIP/glycoprotein/APBA/CNT/BOD electrode was able to facilitate a DET type bioelectrocatalysis for the four-electron reduction of oxygen. That is, the MIP/glycoprotein/APBA/CNT/BOD electrode can act as the biocathode in BFCs. Thus, a miniaturized BFC was fabricated with the assistance of the thionine/graphene/GDH bioanode (**Scheme 2**)**,** where the glycoprotein can be caught by the MIP functional layer on the biocathode surface, due to the recognize interaction between the borate MIP and the glycoprotein. Meanwhile, the APBA/CNT/BOD nanocomposites can capture glycoprotein through the specific interaction between boronate and sugar. Thus, the loading of the APBA/CNT/BOD nanocomposites on the MIP biocathode is directly dependent on the amounts of glycoproteins captured by the MIP biocathode. And the APBA/CNT/BOD nanocomposites is directly related to the oxygen reduction performance of biocathode, and subsequently influence the power output of BFCs. As a result, the amount of the protein can be measured by the change of the current or power output performance of BFC.

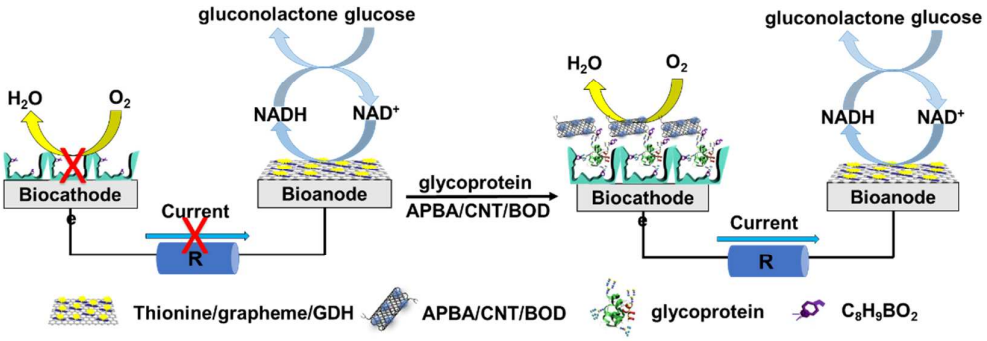

Scheme 2 The principle of the self-powered MIP biosensor for the glycoprotein detection.

The miniaturized BFCs with both the thionine/graphene/GDH anode and MIP-based cathode on a plastic slide was designed, as shown in **Figure 3a**. To decrease the resistance between electrodes, the anode were designed to surround the cathode rather than the parallel to the cathode as our previous work.[13,18] The onset potential for the electrooxidation of glucose is observed at – 0.1 V, and the peak current density reaches a plateau at 140 μA cm^{-2} near 0.2 V. The onset potential for the oxygen electroreduction is observed at 0.51 V and the current density reaches maximum value at 125 μA cm^{-2} near 0.1 V (see **Figure 3b**). These results demonstrate the excellent biocatalytic activities of both bioanode and biocathode, which can promise the high-performance one-compartment BFCs. The control BFCs were also fabricated without MIP template or without BOD or without oxygen or without fuel (see **Figure S4-7**), showing their power output is almost undetectable due to the above four elements are the essential factors for BFCs to work effectively. Meanwhile, BFC without thionine was also measured. It is obvious that thionine plays important role in improving the output of BFCs, since the elimination of the thionine from the anode resulted in the large decrease in the power output (see **Figure S8**).

Figure 3c displays the power curve of the assembled miniaturized glucose/O_2 BFCs after captured HRP in 20 μL HRP (100 μg/mL). The open circuit voltage (V_{oc}) of the cell is estimated to be 615 mV (relative standard deviation (RSD) = 0.7%, n = 8) and the maximum power density (P_{max}) reaches 400 μW cm^{-2} at 400 mV (RSD = 1.3%, n =8). Our miniaturized BFCs can simplify the BFCs fabrication, allow the cell stack up and reduce the cost, showing great potentials in powering the small autonomous sensor-transmitter systems in animals and in plants.

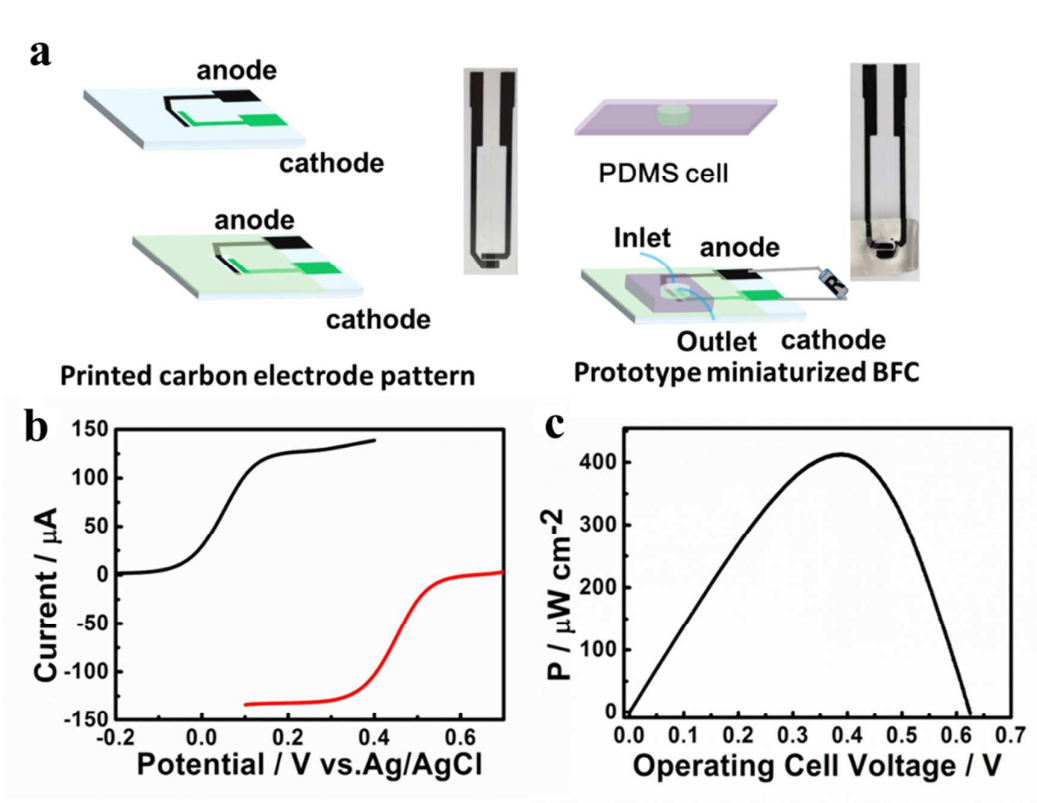

Figure 3 (a) The configuration of BFCs based on the miniaturized imprinted carbon. (b) Polarization curves of the thionine/graphene/GDH anode (black line) and the MIP/HRP/APBA/CNT/BOD cathode (red line). and (c) Dependence of the power density on the cell voltage in air-saturated quiescent solution with 100 μg/mL HRP,

and the electrolyte is 10 mM NAD^+, 15 mM glucose and 0.2 M PBS (pH 7.5) in air-saturated quiescent solution.

3.3. The Optimization. The APBA and BOD concentrations used for the preparation of the cathode probe were optimized to achieve the power maximum (P_{max}) of BFCs. The P_{max} was first examined as a function of the concentration of BOD for the BOD/CNT nanocomposites (**Figure S9**) with the optimal concentration of 20 μM BOD. The P_{max} of the MIP-BFC is reduced after the BOD concentration exceeds 20 μM. This is because the abundant BOD within BOD/CNT nanocomposites disturbs the electron relaying capacity of the CNT, due to the insulting essence of BOD. The effect of the concentration of APBA on the BFCs output was also investigated with a constant amount of enzyme loading **(Figure S10**). The P_{max} of MIP-BFC increases with increasing the concentration of APBA, and reaches a maximum at around 9 μM. The incubation time for the reaction between the BOD/CNT probe and the captured glycoprotein were optimized (**Figure S11**). The incubation time was extremely short (~ 2 min), demonstrating the highly advantageous of the as-prepared sensor compared to the immunoassay, which needs several hours or even overnight for the incubation.

3.4. Measurement of glycoprotein by using the MIP-BFCs-based self-powered sensors. The polarization curves of the sensor in the presence of HRP with various concentrations under the optimal conditions are shown in **Figure 4a**. It is observed that the highest power output value of the cell increases with increasing the HRP

concentration. As shown in Figure 4b, there is a linear relationship between P_{max} and HRP concentration from 1 ng/mL to 10 μg/mL (R_2 = 0.999). As a comparison, a power output for an NIP BFC under otherwise identical conditions is also shown in **Figure 4b**. The imprinting factor for the MIP-BFC is calculated to be 10.9 according to the maximum binding amounts of the MIP-BFC and NIP-BFC obtained from the two curves (**Figure 4b**), thereby confirming the significant binding affinity of the MIP toward the target glycoprotein. The specificity of the boronate-affinity MIP-BFC was first investigated using RNase B (glycoprotein), transferrin (TRF, glycoprotein), bovine serum albumin (BSA, non-glycoprotein), and glucose as interferants. As shown in **Figure 4c**, all the interferants yield the negligible signals at their concentration of 1 mg/mL while the target glycoprotein shows significantly higher signals even at a very low concentration of 1 μg/mL. The cross-reactivity of the HRP-imprinted MIP-BFC toward different proteins was measured (listed in **Table S1**). The highest cross reactivity was 8.2% for ovalbumin (OVA), since its molecular weight (44.3 kDa) is very close to that of HRP (44.2 kDa). Such cross-reactivity is acceptable.

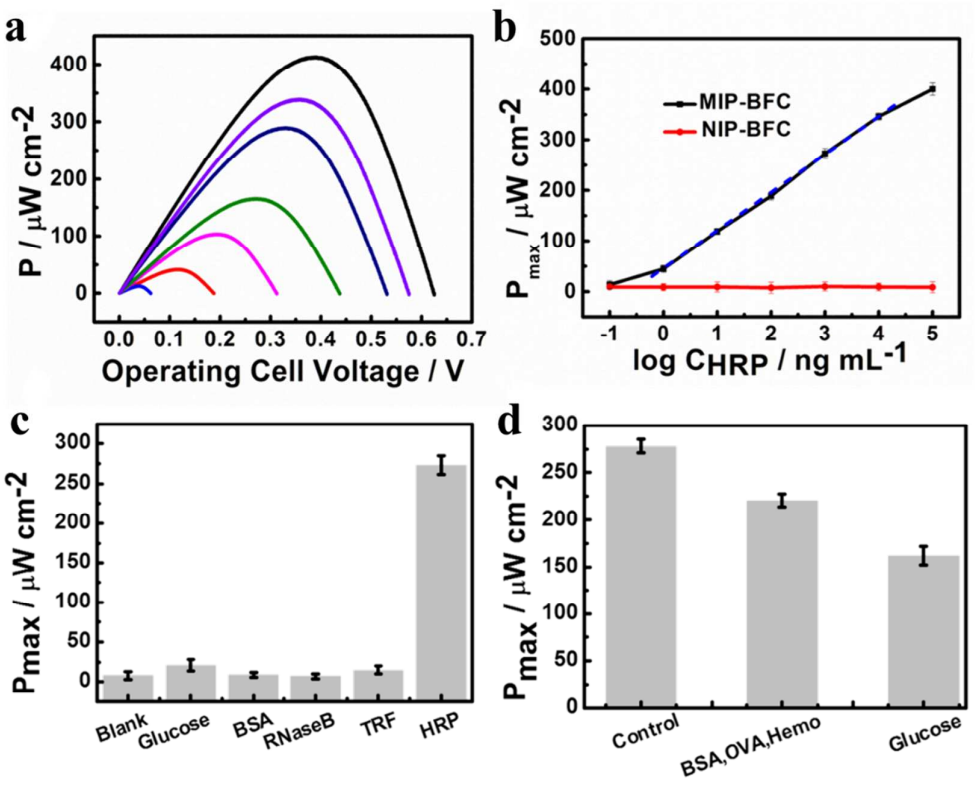

Figure 4 (a) Polarization curves obtained at the miniaturized HRP MIP-BFCs in the presence of HRP with different concentrations at 0.1 ng/mL (blue), 1 ng/mL (red), 10 ng/mL (menga), 100 ng/mL (green), 1 μg/mL (dark blue), 10 μg/mL (purple) and 100 μg/mL (black). Other conditions are the same as those in **Figure 3c**. (b) The relationship (black line) and linearship (blue dash line) between P_{max} and the logarithm of HRP concentrations in MIP-BFCs (black line) and NIP-BFC (red line)-based self-powered sensors. (c) The selectivity of the prepared miniaturized self-powered MIPs-BFCs in the presence of 1 μg/mL HRP or 1 mg/mL interfering protein or 10 mg/mL glucose dissolved in 0.2 M PBS (pH 7.4). The blank sample contains no protein or glucose. (d) The power output of HRP-imprinted MIP-BFC sensor in the presence of additional three interfering agents (1 mg/mL BSA, 1 mg/mL

OVA and 1 mg/mL Hemo) or additional glucose at 10 mg/mL. The control sample is 1 μg/mL HRP in 0.1 M PBS (pH 7.4) without any interference.

The specificity of MIP-BFCs-based self-powered HRP sensor was further evaluated by putting three competing proteins (BSA, OVA and Hemo) into the PBS containing target HRP, and then testing the power output. As shown in **Figure 4d**, MIP-BFCs can still retain 81% of its power output in the presence of three additional competing proteins. Considering OVA is a glycoprotein, having the similar molecular weight with HRP, the selectivity of the self-powered sensor is acceptable. The tolerance of the prepared self-powered MIP-BFCs sensor to the sugar was also examined. The result demonstrates that even in the presence of additional glucose with ten thousand-fold higher concentration (10 mg/mL) than HRP (1 μg/mL), the P_{max} is 43% of the original power output. These results indicate the excellent specificity of the self-powered MIP-BFCs sensor. The reproducibility of the present self-powered MIPs-based sensors was also investigated. The relative standard deviation for 100 ng/mL HRP was about 8.5%.

3.5. Assay of AFP in human serum by MIP-BFCs-based self-powered sensors

The feasibility of the miniaturized MIP-BFCs self-powered sensor for practical clinical applications was demonstrated by an assay of α-fetoprotein (AFP) in human serum, a glycoprotein being routinely used as a biomarker. To carry out the AFP detection, an AFP imprinted MIP-BFC was prepared with the same method using AFP as the imprinted template to establish the self-powered MIP sensor. The obtained AFP MIP-BFCs exhibits a linear response toward AFP within a range from 1 ng/mL

to 1 mg/mL (**Figure 5**). As a comparison, a power output for a non-imprinted polymer (NIP)-BFC under identical conditions is also shown in **Figure 5**. The imprinting factor for the MIP-BFC is calculated to be 9.7 according to the maximum binding amounts of the MIP-BFC and NIP-BFC obtained from the two curves, further confirming the significant binding affinity of the MIP toward the target glycoprotein. Then, serum was first diluted 20-fold and then spiked with AFP of known concentrations. The AFP concentration in the serum from a healthy human is determined to be 12.8 ng/mL by the standard addition method, in good agreement with the result obtained by ELISA method (12.0 ng/mL).[25] The reproducibility of the as-prepared self-powered MIPs-based p53 sensor was also investigated, showing a good relative standard deviation of ~3.2% for 100 ng/mL AFP.

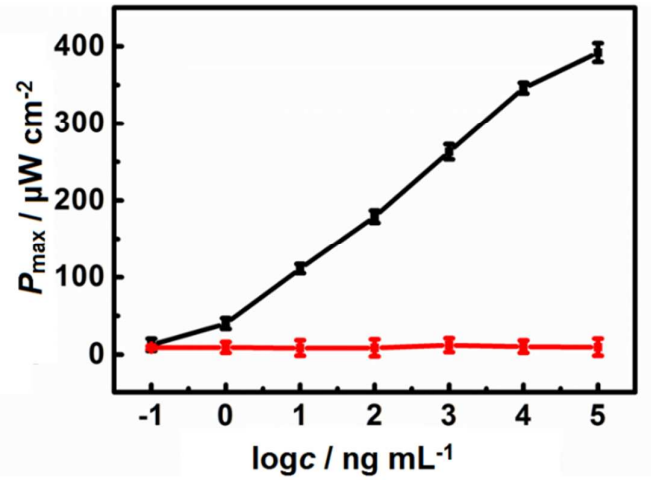

Figure 5 The relationship between P_{max} and the logarithm of AFP concentrations in AFP-imprinted MIP-BFCs (black line) and NIP-BFC (red line)-based self-powered sensors.

4. CONCLUSIONS

In summary, we demonstrate a novel miniaturized BFCs-based self-powered MIP sensor for the highly sensitive and selective detection of glycoproteins by the combination of boronate-affinity MIPs and the boronate-affinity-functionalized BOD/CNT nanocomposites that functionalize as both signal probe and biocatalyst at the cathode. We found that the maximum power density of the MIP-based BFC is highly dependent on the amount of BOD label in the biocathode, thus the added amount of target analyte. The boronate-affinity MIP ensures the specificity, along with the self-powered biosensor based on the BFCs detection guarantees the sensitivity. Under such new sensing mechanism, our self-powered BFCs-based MIP sensor shows a wide linear range for the detection of HRP from 1 ng/mL to 10 μg/mL with a low detection limit of 1 ng/mL. The prepared self-powered MIP biosensor also exhibits high tolerance for different interferences, such as sugar or other glycoproteins. To demonstrate the clinical relevance of our biosensors, the level of AFP in serum samples were measured be around 12.8 ng/mL, being well in accordance with those from the ELISA analysis. The as-prepared self-powered MIP sensor exhibits significant advantages over a conventional immunoassay in terms of cost efficiency, stability and speed. Furthermore, the present miniaturized self-powered MIP-based sensor can be accomplished only *via* a multimeter without the need of any large and expensive instruments in laboratories, which provide a simple, economical, sensitive, and portable device for point-of-care and on-site applications.

■ ASSOCIATED CONTENT

* Supporting Information

The Supporting Information is available free of charge on the ACS Publications website at http://pubs.acs.org.

Additional figures including TEM images, SEM images, CV curves of electrode in different condition, current-potential curves, the optimization curves and tables of cross-reactivity of MIPs-BFCs for HRP toward different proteins.

■ AUTHOR INFORMATION

Corresponding Authors

*E-mail: dengliu@csu.edu.cn (L. Deng)

*E-mail: liuyounian@csu.edu.cn (Y.-N. Liu), Phone/Fax: +86-731-8887 9616

Notes

The authors declare no competing financial interest.

■ ACKNOWLEDGMENTS

This work was financially supported by National Natural Science Foundation of China (Nos. 21105126, 21476266 and 21276285).

■ REFERENCES

(1) Peschke, M.; Moog, D.; Klingl, A.; Maier, U. G.; Hempel, F. Evidence for Glycoprotein Transport into Complex Plastids. *Proc. Nat. Acad. Sci. USA* **2013**, 110, 10860–10865.

(2) Yang, N.; Feng, S.; Shedden, K.; Xie, X.; Liu, Y.; Rosser, C. J.; Lubman, D. M.; Goodison, S. Urinary Glycoprotein Biomarker Discovery for Bladder Cancer Detection Using LC/MS-MS and Label-Free Quantification. *Cancer Res*. **2011**, 17, 3349–3359.

(3) Georges, E.; Bradley, G.; Gariepy, J.; Ling, V. Detection of P-Glycoprotein Isoforms by Gene-Specific Monoclonal Antibodies. *Proc. Nat. Acad. Sci.* **1990**, 87, 152–156.

(4) Cong, W. T.; Zhou, A. Y.; Liu, Z. G.; Shen, J. Y.; Zhou, X.; Ye, W. J.; Zhu, Z. X.; Zhu, X. L.; Lin, J. J.; Jin, L. T. Highly Sensitive Method for Specific, Brief, and Economical Detection of Glycoproteins in Sodium Dodecyl Sulfate-Polyacrylamide Gel Electrophoresis by the Synthesis of a New Hydrazide Derivative. *Anal. Chem*. **2015**, 87, 1462–1465.

(5) Stavenhagen, K.; Hinneburg, H.; Thaysen-Andersen, M.; Hartmann, L.; Silva, D. V.; Fuchser, J.; Kaspar, S.; Rapp, E.; Seeberger, P. H.; Kolarich, D. Quantitative Mapping of Glycoprotein Micro-Heterogeneity and Macro-Heterogeneity: An Evaluation of Mass Spectrometry Signal Strengths Using Synthetic Peptides and Glycopeptides. *J. Mass Spectrom*. **2013**, 48, 627-639.

(6) Zhang, H. L.; Wei, X. L.; Zang, Y.; Cao, J. Y.; Liu, S.; He, X. P.; Chen, Q.; Long, Y. T.; Li, J.; Chen, G. R. Fluorogenic Probing of Specific Recognitions Between Sugar Ligands and Glycoprotein Receptors on Cancer Cells by an Economic Graphene Nanocomposite. *Adv. Mater*. **2013**, 25, 4097–4101.

(7) Zhou, M.; Dong, S. J. Bioelectrochemical Interface Engineering: Toward the Fabrication of Electrochemical Biosensors, Biofuel Cells, and Self-Powered Logic Biosensors. *Acc. Chem. Res*. **2011**, 44, 1232–1243.

(8) Ravenna, Y.; Xia, L.; Gun, J.; Mikhaylov, A. A.; Medvedev, A. G.; Lev, O.; Alfonta, L. Biocomposite Based on Reduced Graphene Oxide Film Modified with

Phenothiazone and Flavin Adenine Dinucleotide-Dependent Glucose Dehydrogenase for Glucose Sensing and Biofuel Cell Applications. *Anal. Chem.,* **2015**, 87, 9567–9571.

(9) Han, Y., Chabu, J. M., Hu, S., Deng, L., Liu, Y. -N., Guo, S. J. Rational Tuning of the Electrocatalytic Nanobiointerface for a "Turn-Off" Biofuel Cell Based Self-Powered Biosensor for P53 Protein. *Chem. -Eur. J.* **2015**, 21, 13045-13051.

(10) Asghary, M., Raoof, J. B., Rahimnejad, M., Ojani, R. A Novel Self-Powered and Sensitive Label-Free DNA Biosensor in Microbial Fuel Cell. *Biosens. Bioelectron.* **2016**, 82, 173-176.

(11) Katz, E.; Bückmann, A. F.; Willner, I. Self-Powered Enzyme-Based Biosensors. *J. Am. Chem. Soc.* **2001**, 123, 10752–10753.

(12) Hou, C. T.; Fan, S. Q.; Lang, Q. L.; Liu, A. H. Biofuel Cell Based Self-Powered Sensing Platform for L-Cysteine Detection. *Anal. Chem.* **2015**, 87, 3382–3387.

(13) Deng, L.; Chen, C. G.; Zhou, M.; Guo, S. J.; Wang, E. K.; Dong, S. J. Integrated Self-Powered Microchip Biosensor for Endogenous Biological Cyanide. *Anal. Chem.* **2010**, 82, 4283–4287.

(14) Zhang, L. L.; Zhou, M.; Dong, S. J. A Self-Powered Acetaldehyde Sensor Based on Biofuel Cell. *Anal. Chem.* **2012**, 84, 10345–10349.

(15) Gai, P., Song, R., Zhu, C., Ji, Y., Wang, W., Zhang, J. R., Zhu, J. J. Ultrasensitive Self-Powered Cytosensors Based on Exogenous Redox-Free Enzyme Biofuel Cells as Point-of-Care Tools for Early Cancer Diagnosis. *Chem. Commun.* **2015**, 51, 16763–16766.

(16) Germain, M. N.; Arechederra, R. L.; Minteer, S. D. Nitroaromatic Actuation of Mitochondrial Bioelectrocatalysis for Self-Powered Explosive Sensors. *J. Am. Chem. Soc*. **2008**, 130, 15272–15273.

(17) Wang, Y. H.; Ge, L.; Wang, P. P.; Yan, M.; Yu, J. H.; Ge, S. G. A Three-Dimensional Origami-Based Immuno-Biofuel Cell for Self-Powered, Low-Cost, and Sensitive Point-of-Care Testing. *Chem. Commun.* **2014**, 50, 1947–1949.

(18) Chen, J. S.; Han, Y. J.; Deng, L.; Guo, S. J. Carbon Nanotube–Bilirubin Oxidase Bioconjugate as a New Biofuel Cell Label for Self-Powered Immunosensor. *Anal Chem*. **2014**, 86, 11782–11788.

(19) Tam, T. K.; Strack, G.; Pita, M.; Katz, E. J. Biofuel Cell Logically Controlled by Antigen-Antibody Recognition: Towards Immune-Regulated Bioelectronic Devices. *J. Am. Chem. Soc*. **2009**, 131, 11670–11671.

(20) Wang, Y. H.; Ge, L.; Ma, C.; Kong, Q. K.; Yan, M.; Ge, S. G.; Yu, J. H. Self-Powered and Sensitive DNA Detection in a Three-Dimensional Origami-Based Biofuel Cell Based on a Porous Pt-Paper Cathode. *Chem. Eur. J.* **2014**, 20, 12453–12462.

(21) Zhou, M.; Du, Y.; Chen, C. G.; Li, B. L.; Wen, D.; Dong, S. J.; Wang, E. K. Aptamer-Controlled Biofuel Cells in Logic Systems and Used as Self-Powered and Intelligent Logic Aptasensors. *J. Am. Chem. Soc*. **2010**, 132, 2172–2174.

(22) Li, W.; Sun, Y.; Yang, C. C.; Yan, X. M.; Guo, H.; Fu, G. Q. Fabrication of Surface Protein-Imprinted Nanoparticles Using a Metal Chelating Monomer via

Aqueous Precipitation Polymerization. *ACS Appl. Mater. Interfaces,* **2015***,* 7, 27188–27196.

(23) Ye, J.; Chen, Y.; Liu, Z. A Boronate Affinity Sandwich Assay: An Appealing Alternative to Immunoassays for the Determination of Glycoproteins. *Angew. Chem. Int. Ed.* **2014**, 53, 10386–10389.

(24) Li, L.; Lu, Y.; Bie, Z.; Chen, H. Y.; Liu, Z. Photolithographic Boronate Affinity Molecular Imprinting: A General and Facile Approach for Glycoprotein Imprinting. *Angew. Chem. Int. Ed,* **2013**, 52, 7451-7454.

(25) Pan, X. H.; Chen, Y.; Zhao, P. X.; Li, D. J.; Liu, Z. Highly Efficient Solid-Phase Labeling of Saccharides within Boronic Acid Functionalized Mesoporous Silica Nanoparticles. *Angew. Chem. Int. Ed*. **2015**, 54, 6271–6274.

(26) Zhang, W.; Liu, W.; Li, P.; Xiao, H.; Wang, H.; Tang, B. A Fluorescence Nanosensor for Glycoproteins with Activity Based on the Molecularly Imprinted Spatial Structure of the Target and Boronate Affinit. *Angew. Chem. Int. Ed.* **2014**, 53, 12697–12701.

(27) Yan, Y.; Zheng, W.; Su, L.; Mao, L. Carbon-Nanotube-Based Glucose/O_2 Biofuel Cells. *Adv. Mater.* **2006**, 18, 2639–2642.

(28) Sun, Z.; Fu, H.; Deng, L.; Wang, J. Redox-Active Thionine–Graphene Oxide Hybrid Nanosheet: One-Pot, Rapid Synthesis, and Application as a Sensing Platform for Uric Acid. *Anal. Chem. Acta,* **2013**, 761, 84-91.

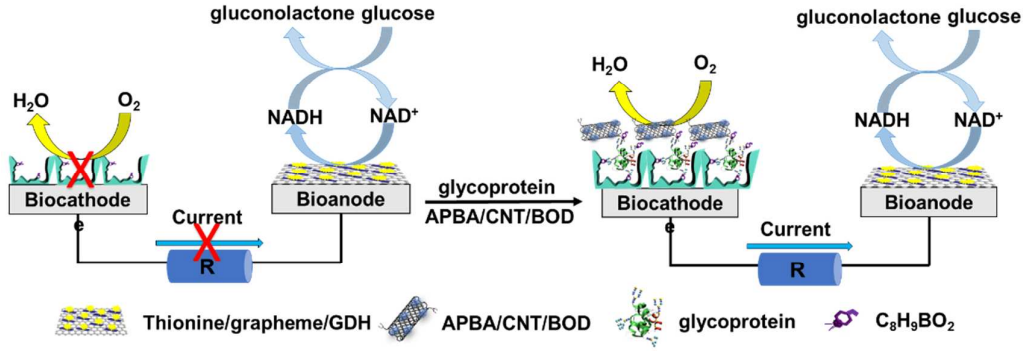
gluconolactone glucose
H_2O
O_2
NADH
NAD^+
Biocathode
Bioanode
Current
R
e
glycoprotein
APBA/CNT/BOD
Thionine/grapheme/GDH
APBA/CNT/BOD
glycoprotein
$C_8H_9BO_2$

TOC

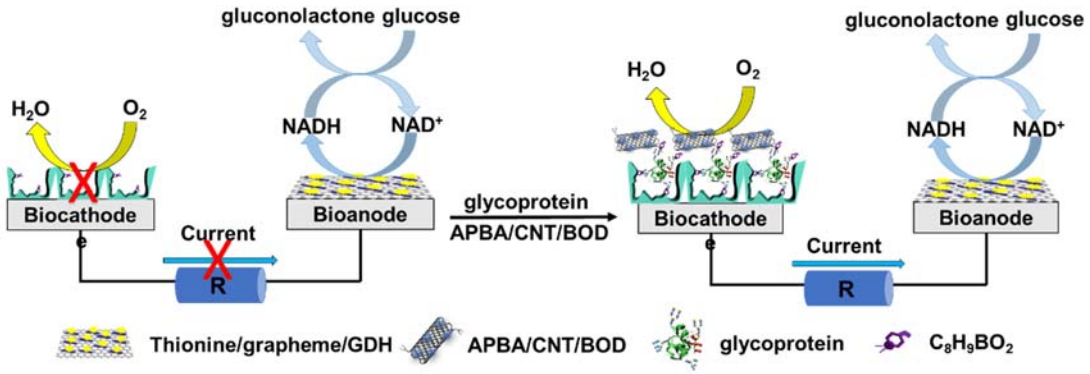
gluconolactone glucose
H_2O
O_2
NADH
NAD^+
Biocathode
Bioanode
Current
R
e
glycoprotein
APBA/CNT/BOD
Thionine/grapheme/GDH
APBA/CNT/BOD
glycoprotein
$C_8H_9BO_2$

TOC